▌**Laser Chemistry**

# Laser Access to Quercetin Radicals and Their Repair by Co-antioxidants

Tim Kohlmann and Martin Goez*[a]

**Abstract:** We have demonstrated the feasibility and ease of producing quercetin radicals by photoionization with a pulsed 355 nm laser. A conversion efficiency into radicals of 0.4 is routinely achieved throughout the pH range investigated (pH 2–9), and the radical generation is completed within a few ns. No precursor other than the parent compound is needed, and the ionization by-products do not interfere with the further fate of the radicals. With this generation method, we have characterized the quercetin radicals and studied the kinetics of their repairs by co-antioxidants such as ascorbate and 4-aminophenol. Bell-shaped pH de-

pendences of the observed rate constants reflect opposite trends in the availability of the reacting protonation forms of radical and co-antioxidant and even at their maxima mask the much higher true rate constants. Kinetic isotope effects identify the repairs as proton-coupled electron transfers. An examination of which co-antioxidants are capable of repairing the quercetin radicals and which are not confines the bond dissociation energies of quercetin and its monoanion experimentally to 75–77 kcal mol$^{-1}$ and 72–75 kcal mol$^{-1}$, a much narrower interval in the case of the former than previously estimated by theoretical calculations.

## Introduction

Quercetin (for the structural formula see Scheme 2) is one of the most abundant representatives of the flavonoid antioxidants, a subgroup of the polyphenols, and boasts of an activity four times as high as that of $\alpha$-tocopherol (vitamin E) or ascorbate (vitamin C).[1] An impressive collection of other health benefits has been reported, including antihypertensive,[2] cardioprotective,[3] antithrombotic as well as anti-inflammatory,[4] antitumor,[5] and antiviral effects, the latter in particular against RNA viruses such as SARS-CoV,[6] MERS-CoV,[7] Ebola-CoV,[8] Zika-CoV,[9] and possibly SARS-CoV-2.[10]

The oral bioavailability of quercetin is severely limited by its low solubility in water, hence carriers[6] or glucosylation[7–9] have been tested to overcome that limitation. An alternative strategy—although the link between the antioxidative and the other health-protecting properties of quercetin is not clearly proven yet—is provided by redox cycling with the aid of a hydrophilic co-antioxidant exhibiting higher plasma levels such as ascorbate, which repairs the oxidized quercetin radicals.

There is indeed evidence that the antioxidant activity of quercetin is substantially improved by,[11] and that its antitumor and antiviral potency even relies crucially on,[12,13] the presence of ascorbate. Yet, and despite nearly 80 000 publications on quercetin listed by SciFinder to date, very little is known about the repair of its radicals by ascorbate and related co-antioxidants. Practically all such investigations were carried out through incubation experiments on long timescales,[14] which inherently can only yield indirect information on the fast processes and are prone to interpretational ambiguities because the quercetin oxidation products may themselves function as secondary antioxidants.[15–17] To our knowledge, there have only been two kinetic studies on short timescales;[18,19] and both used pulse radiolysis with its innate problems of delayed quercetin radical generation through scavenging, as well as a considerable number of transients and reactions interacting simultaneously.

Herein, we explore an alternative approach, which we have already successfully applied to the antioxidant resveratrol,[20] namely, direct generation of the quercetin radicals by laser-induced photoionization. As we will show, this access to the radicals is not only completely selective over a wide pH range but also quasi-instantaneous compared to the subsequent reactions of the radicals, such that the repair kinetics can be observed in isolation, their complicated pH dependence can be unravelled, and the bond dissociation energy of quercetin can be bracketed experimentally with a significantly lower uncertainty compared to reported quantum-mechanical estimates.

[a] *T. Kohlmann, Prof. Dr. M. Goez*
*Martin-Luther-Universität Halle-Wittenberg*
*Institut für Chemie*
*Kurt-Mothes-Str. 2, 06120 Halle (Saale) (Germany)*
*E-mail: martin.goez@chemie.uni-halle.de*

🄳 *The ORCID identification number(s) for the author(s) of this article can be found under:*
*https://doi.org/10.1002/chem.202001956.*

## Experimental Section

All chemicals were used as received in the purity specified by the manufacturer (Sigma–Aldrich; quercetin, >96%; sodium ascorbate,

**Chemistry–A European Journal**

Full Paper
doi.org/10.1002/chem.202001956

**Chemistry Europe**
European Chemical
Societies Publishing

≥99.0%; ascorbic acid, ≥99.7%; 4-aminophenol, >98%; Trolox, 97%; hydroquinone, >98%; NaOH, 99%; HCl, 99%). The solvent was ultrapure Millipore Milli-Q water (specific resistance, 18.2 M$\Omega$ cm$^{-1}$) or—for measuring the H/D kinetic isotope effects—D$_2$O (99.9% deuteration, DEUTERO).

The solutions were deoxygenated with argon, or with N$_2$O when the hydrated electron had to be blanked out as explained in the main text, for at least 30 minutes. Both gases were of purity 5.0 and obtained from AirLiquide. The quercetin weight-in concentration was 5 $\mu$M throughout, which kept the solutions optically thin and thus avoided filter effects caused by nonlinear absorption. The desired pH values were adjusted under pH meter control by the addition of NaOH or HCl. All measurements were carried out at room temperature.

Mechanistic and kinetic experiments studies were performed on a home-made laser flash photolysis setup described elsewhere.[21] Its main characteristics pertinent to this investigation are excitation with a frequency-tripled (355 nm) pulsed Nd:YAG laser (Continuum Surelite-III; pulse width, ca. 5 ns); homogeneous illumination of the observed volume (window, 2×4 mm; optical path length, 4 mm) in a suprasil flow cell; detection at right angles to the excitation beam and with a time resolution down to 1 ns.

The steady-state absorption and the fluorescence spectra were recorded on a Shimadzu UV-1800 spectrophotometer and an Edinburgh Instruments FS5 TCSPC spectrometer.

## Results and Discussion

### Access to the quercetin radicals

Figure 1 focuses on the photophysics of quercetin as far as is essential for this work. The antioxidant exists in five protonation states with typical separations between p$K_a$ values by less than 2 units,[22] which is comparable to the spread of the reported individual values (e.g., between 5.50 and 7.65 for the lowest p$K_a$).[22,23] Herein, only the fully protonated and singly deprotonated forms H$_2$Q and HQ$^-$ (for the structures see the summarizing Scheme 2) play a role because we observed sample deterioration above pH 9 on the timescale of 1–2 h, which restricted the pH range accessible to our experiments.

The complexity of the system is reflected by the pH-dependent absorption spectra of Figure 1a, which exhibit no well-defined isosbestic points; however, 376 nm provides a good approximation of such a point up to pH≈8.5, i.e., except for the highest pH in Figure 1. Excitation at 376 nm thus allowed recording the fluorescence spectra (Figure 1b) with no, or only a minor (≈7%) correction. At the wavelength of our ionizing laser, 355 nm, the profile displayed as the inset of Figure 1a can be fitted with a titration curve with a p$K_a$ of 7.5, although no plateau value is reached at the high-pH end of the region. The observed ground-state extinction coefficient $\varepsilon_{GS}$ decreases by about one third when going from pH 4 to pH 9. This reduces the rate of excitation by our laser in proportion but does not cause sensitivity problems because $\varepsilon_{GS}$ is still quite high in the basic medium.

The absorption-corrected fluorescence spectra of Figure 1b clearly show a weakly emitting species at lower pH and a much more strongly emitting species at higher pH, with emission maxima at 521 nm and 554 nm. A profile at the longer wavelength (see, inset of the Figure) is represented well by a titration curve with a p$K_a$ of 7.3. On account of the distinct and complete curve shape, we regard this p$K_a$—which hardly differs from the above one—as reliable; and we interpret the data of Figure 1 by absorption of, and emission from, the same protonation state, the concentration of which is determined by the ground-state equilibrium between H$_2$Q and HQ$^-$, with pertaining p$K_a$ of 7.3. Phenols are more acidic in the excited S$_1$ state compared to the ground state;[24] hence, the obvious absence of proton transfer in the excited state points to a very short S$_1$ lifetime.

Laser flash photolysis at 355 nm affords transient spectra that can be decomposed into the spectral signatures displayed in Figure 2a. The occurrence of the hydrated electron e$_{aq}^{\bullet-}$ is evidenced by its characteristic strong and broad absorption with maximum at about 720 nm, and by the fact that this spectral feature is absent when the solution has been saturated with the specific e$_{aq}^{\bullet-}$ scavenger N$_2$O or when the pH lies below about 2. Both N$_2$O and H$^+$ are known to react diffusion-con-
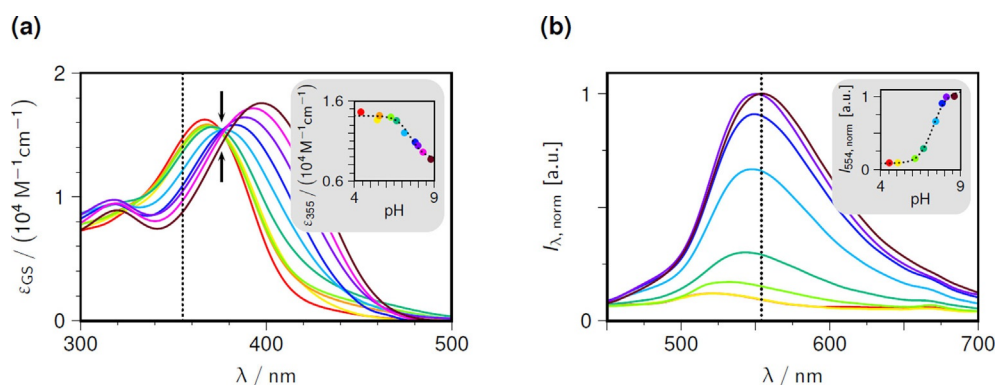


**Figure 1.** Photophysics of quercetin (5.05 $\mu$M) in homogeneous aqueous solution at different pH (between 4.4 and 8.8; identical colour coding between inset and main plot of each subfigure). Graph (a): main plot, ground-state absorption spectra, with the dotted line and the arrows indicating our photoionization wavelength (355 nm) and the approximate isosbestic point (376 nm); inset, pH dependence of the observed extinction coefficient at 355 nm, with the dotted best-fit titration curve corresponding to a p$K_a$ of 7.5. Graph (b): main plot, fluorescence spectra upon excitation at 376 nm, after pH-dependent correction for $\varepsilon_{376}$ and normalization to the maximum (554 nm) at the highest pH; inset, profile at 554 nm (as indicated by the dotted line in the main plot), with dotted best-fit titration curve yielding a p$K_a$ of 7.3. For further explanation, see the text.

**Chemistry–A European Journal**

Full Paper
doi.org/10.1002/chem.202001956

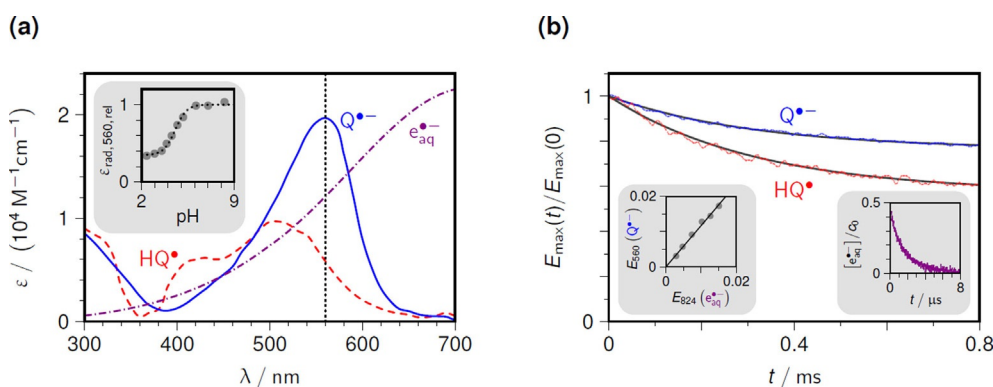**Chemistry Europe**
European Chemical
Societies Publishing

**Figure 2.** Characterization of the intermediates (radical anion $Q^{\bullet-}$, blue; neutral radical $HQ^{\bullet}$, red; hydrated electron $e_{aq}^{\bullet-}$,[26] violet) following quercetin photoionization in homogeneous aqueous solution. Graph (a): main plot, calibrated absorption spectra corrected for absorption of the starting quercetin; inset, pH dependence of the apparent extinction coefficient of the quercetin radicals at 560 nm ($pK_a = 4.5$, from the dotted best-fit titration curve). Graph (b): main plot, slow decays of the relative absorptions at 560 nm of $Q^{\bullet-}$ (pH 8.2) and $HQ^{\bullet}$ (pH 2.3) superimposed on monoexponential fits (gray curves) with global rate constant of $1/(320 \, \mu s)$ and local end values of 0.76 and 0.57; right inset, fast $e_{aq}^{\bullet-}$ decay (pH 8.2) from a starting concentration $c_0$ of about 2.2 μM; left inset, illustration of the spectral calibration of $Q^{\bullet-}$ at pH 8.2 by comparing the initial extinctions $E$ of $Q^{\bullet-}$ at 560 nm and of $e_{aq}^{\bullet-}$ at 824 nm. For further explanation, see the text.

trolled with $e_{aq}^{\bullet-}$ to give the nonabsorbing radicals HO$^{\bullet}$ and H$^{\bullet}$;[25] and under the described conditions the life of $e_{aq}^{\bullet-}$ is shortened so much (to a few ns, which is the duration of our laser pulses) as to render it undetectable. These observations thus identify the laser-induced process as a photoionization.

When $e_{aq}^{\bullet-}$ is blanked out by N$_2$O saturation, the transient spectra of the accompanying quercetin-derived radicals are obtained in pure form because any subsequent attack of HO$^{\bullet}$ on residual HQ$^{\bullet}$ or H$_2$Q affords the same radical as the photoionization does.[27] By the two independent procedures described below, we calibrated the spectra and corrected them for depletion of the starting quercetin (Figure 2a). In accordance with a pulse-radiolytic study and a theoretical investigation, which concluded that the radical cation initially resulting from H$_2$Q is deprotonated quasi-instantaneously,[19,28] the limiting spectra at the low and high ends of our pH range are assigned to the neutral radical HQ$^{\bullet}$ and the radical anion Q$^{\bullet-}$ (see Scheme 2). Compared to the previously reported experimental results,[19] we find a similar $pK_a$ of HQ$^{\bullet}$ (4.5, i.e., higher by 0.3 units) but much higher extinction cooefficients at maximum ($19750 \, M^{-1} \, cm^{-1}$ and $9700 \, M^{-1} \, cm^{-1}$ for Q$^{\bullet-}$ and HQ$^{\bullet}$, i.e., higher by factors of about 2 and 4). These observations strongly suggest the spectral calibration as the origin of the discrepancies because a calibration error will additionally distort the weaker and hypsochromic absorption of HQ$^{\bullet}$ (maximum at 510 nm, i.e., in the outer wing of the longest-wavelength bands in Figure 1a) through depletion of the starting quercetin, whereas that effect is absent for the stronger and bathochromic absorption of Q$^{\bullet-}$ (maximum at 560 nm); and calibration errors cancel to first order in the $pK_a$ determination at the maximum of the Q$^{\bullet-}$ band.

Figure 2b addresses the post-generation fate of the transients. Both HQ$^{\bullet}$ and Q$^{\bullet-}$ are seen to be intrinsically long-lived intermediates that decay on the timescale of a few hundreds of μs to give other absorbing species. A successful global fit of a first-order kinetic model indicates that the rate constants of these transformations are independent of pH, and that the ex-

tinction coefficients of the products are similar to, but slightly smaller than, those of Q$^{\bullet-}$ and HQ$^{\bullet}$, respectively. The products are most likely different protonation states of the structure displayed at the lower right in Scheme 2,[29] but further characterization was not warranted because these conversions fall outside the temporal window of the repair reactions by our co-antioxidants.

In contrast to the quercetin-derived radicals, the natural decay of $e_{aq}^{\bullet-}$ occurs within a few μs in basic medium (see, right inset of the Figure) and increasingly more rapidly when the pH is lowered. This has two implications. On one hand, an attack of $e_{aq}^{\bullet-}$ on H$_2$Q or HQ$^-$ plays no role in this work because the μM concentrations render these reactions noncompetitive; and the same holds true for HO$^{\bullet}$ when N$_2$O saturation is employed, or for H$^{\bullet}$ when $e_{aq}^{\bullet-}$ is generated in acidic medium. On the other hand, down to about pH 3 the life of $e_{aq}^{\bullet-}$ is long enough for precise determinations of the initial post-flash concentrations, which in turn provides the basis for our first calibration procedure: On the premise that the ejection of $e_{aq}^{\bullet-}$ is the only pathway to the quercetin radicals, stoichiometric equivalence demands a proportionality between the ratio of the extinctions and that of the extinction coefficients. The possibility of blanking out $e_{aq}^{\bullet-}$ makes this a trivial task. First, the superposition of the absorptions of $e_{aq}^{\bullet-}$ plus HQ$^{\bullet}$ and/or Q$^{\bullet-}$ is recorded in argon-saturated solution; then, N$_2$O saturation is used to record only the absorptions of the quercetin radicals; and a difference of the two measurements yields the pure $e_{aq}^{\bullet-}$ absorption. The concentrations of the transients are varied most conveniently through the laser intensity. The left inset of Figure 2b illustrates the proportionality for the spectral maximum of Q$^{\bullet-}$ (560 nm) and a convenient wavelength for $e_{aq}^{\bullet-}$ (not the 720 nm maximum but 824 nm, entirely for technical reasons).[30]

Obviously, the validity of this calibration approach hinges on the absence of homolytic photodissociation of the O–H bond as a major pathway to the quercetin radicals that bypasses photoionization. However, this assumption is very reasonable

Chemistry–A European Journal

**Full Paper**
doi.org/10.1002/chem.202001956

**Chemistry
Europe**
European Chemical
Societies Publishing

because for phenols in water the quantum yields of such homolyses are known to be practically zero.[31] This is corroborated by juxtaposing the photolyses at pH 5.8 and pH 8.2. These start out near quantitatively from $H_2Q$ and from $HQ^-$ (including their $S_1$ states as discussed above), and despite significantly different bond dissociation energies (according to the literature: $77.2 \pm 5.9$ kcal mol$^{-1}$ for $H_2Q$;[28,32–35] and $73.0 \pm 2.1$ kcal mol$^{-1}$ for $HQ^-$)[28,32,35] yield practically the same calibrated extinction coefficient of $Q^{•-}$ (with $HQ^•$ accounting for less than 5% in both experiments). It is also vindicated by our second calibration procedure (see next section).

Figure 3 finally deals with the efficiency of the photoionization access to the quercetin radicals. The intensity dependences of the $e_{aq}^{•-}$ concentrations (main plot) show that more than 40% of the starting quercetin can be converted into radicals by a single laser pulse, meaning that radical concentrations of 2 μM are routinely attainable in situ and within 5 ns. Surprisingly, the protonation state of the quercetin plays only an insignificant role: at given laser intensity, $H_2Q$ (at pH 5) and $HQ^-$ (above pH 8) afford $e_{aq}^{•-}$ concentrations that are so similar as to fall nearly within the margin of experimental error.

Phenol(ate) ionizations are known to be biphotonic.[31] In apparent opposition, no dependence of the $e_{aq}^{•-}$ yield on the square of the laser intensity is discernible, but it is well understood that unfavourable combinations of parameters often prevent a clear manifestation of this limiting relationship.[30,36] As the best-fit curve to a biphotonic ionization model in the main plot of Figure 3 shows, the validity of the quadratic approximation is restricted to an almost imperceptibly small range near the origin. More importantly, the fit converges on complete ionization at infinite intensity, in other words, suggests that homolytic dissociation of the phenolate O–H bond is absent under our conditions, which further supports our above calibration of the extinction coefficients of the quercetin radicals.

The unexpectedly negligible influence on the $e_{aq}^{•-}$ yield of the decrease of the ground-state extinction coefficient by 30% when going from $HQ^-$ to $H_2Q$ is revealed most clearly by the
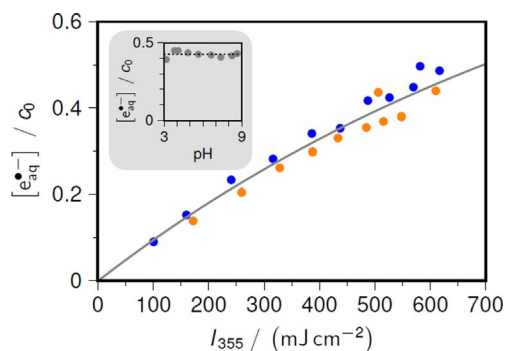


**Figure 3.** Photoionization process of quercetin in homogeneous aqueous solution. Main plot, dependence of the $e_{aq}^{•-}$ yields relative to the quercetin weight-in concentration $c_0$ (5 μM) on the laser intensity $I_{355}$. Blue data points, pH 8.1; orange data points, pH 5.0. The solid curve is the fit of a biphotonic model to all data; best-fit limiting $e_{aq}^{•-}$ yield at infinite intensity, 100%; other fit parameters without relevance. Inset, pH dependence of relative $e_{aq}^{•-}$ yield at $I_{355} = 507$ mJ cm$^{-2}$. For further explanation, see the text.

absence of a pH dependence at constant laser intensity in the inset of the Figure. The reason must be an accidental cancellation by different extinction coefficients of, lifetimes of, and photodetachment efficiencies from, the excited states of $H_2Q$ and $HQ^-$. All these parameters are inaccessible to our experiments on ns timescales, but in the context of this work, their knowledge is also irrelevant. It is sufficient that photoionization of quercetin, regardless of whether it is present as $H_2Q$ or $HQ^-$, with a 355 nm laser provides a direct access to useable concentrations of quercetin radicals, as the experiments of this section have demonstrated and Scheme 2 at the end of this "Results and Discussion" section sums up.

## Repair reactions by co-antioxidants

Whereas transformations of $HQ^•$ and/or $Q^{•-}$ on their own are hardly noticeable during the first 20 μs after the generating laser flash, the addition of the archetypal co-antioxidant ascorbate changes the situation. Figure 4a epitomizes the effects, on which our second procedure for calibrating the extinction coefficients of the quercetin radicals is based.

The experimental pH of 6.5 ensures a single protonation state for the quercetin radicals and for the ascorbate, namely, $Q^{•-}$ and the monoanion $HAsc^-$ (compare Scheme 1; $HAsc^-$ is completely transparent above 320 nm). The same condition is fulfilled for the ascorbyl radical $Asc^{•-}$ (Scheme 1), which has an absorption maximum at 360 nm with an extinction coefficient of 4500 M$^{-1}$ cm$^{-1}$.[26] Best suited for observation at this pH are thus 560 nm (maximum of the $Q^{•-}$ absorption) and 360 nm. The former wavelength responds to $Q^{•-}$ only whereas the latter captures $Q^{•-}$, depletion of quercetin, and $Asc^{•-}$.

We stress that all three contributions are already present directly after the laser flash, i.e., at 0 μs: because the experiment is performed in $N_2O$ saturated solution, $e_{aq}^{•-}$ yields $HO^•$ within nanoseconds; in turn, $HO^•$ is scavenged even faster by the high concentration of $HAsc^-$ (100 mM) to give $Asc^{•-}$; in sum, $e_{aq}^{•-}$ is thus quantitatively and quasi-instantaneously converted into $Asc^{•-}$. Experimental proof is provided by comparing the initial absorption at 360 nm, which deceptively lies near zero, with that in a control experiment without $HAsc^-$ but under otherwise identical conditions. The negative and persistent transient absorption in the control experiment reveals the true contributions of $Q^{•-}$ and quercetin depletion. In the experiment with ascorbate, a transient spectrum after 15 μs is completely dominated by the band of $Asc^{•-}$, which identifies the main reaction as the repair of the quercetin radical, in accordance with expectation.

The absorption trace at 560 nm does not decay to zero but to a small residual value, about 4% of the initial absorption, on account of the competition of the repair with the natural conversion of $Q^{•-}$ into an unspecified absorbing product (compare, Figure 2b). However, at 360 nm that product and $Q^{•-}$ must have practically the same extinction coefficient, as is evident from the constant absorption trace in the control experiment. After the straightforward and very small corrections for the described side reaction, the final absorption at 360 nm in the experiment with ascorbate is proportional to twice the extinction
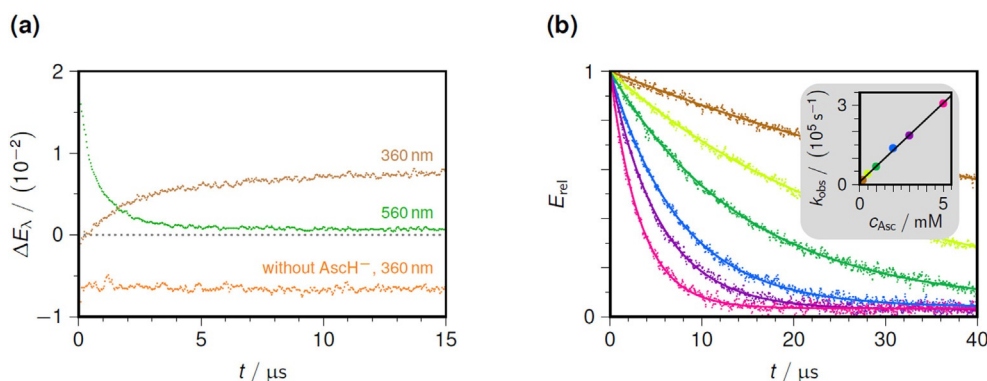
**Chemistry–A European Journal**

Full Paper
doi.org/10.1002/chem.202001956

**Chemistry Europe**
European Chemical
Societies Publishing

**Figure 4.** Repair of the quercetin radical (about 2.1 μM) by ascorbate in homogeneous aqueous solution saturated with $N_2O$. Graph (a): extinction traces $\Delta E$ used for calibrating $\varepsilon_{max}$ of $Q^{\bullet-}$; pH 6.5; ascorbate weight-in concentration, 100 mM and 0 mM (control experiment). Green trace, 560 nm; detection of $Q^{\bullet-}$. Brown and orange traces, 360 nm; superposition of (starting) quercetin depletion, $Q^{\bullet-}$ decay, and $Asc^{\bullet-}$ formation (not in the control experiment without ascorbate). The dotted gray line ($\Delta E = 0$) serves to guide the eye. Graph (b): dependence of the observed repair rate constant $k_{obs}$ on the ascorbate weight-in concentration $c_{Asc}$ (color-coded identically in the main plot and the inset) at pH 4.25. Main plot, decay curves of the quercetin radicals, measured through the extinctions $E_{rel}$ (at 515 nm, each curve normalized to the initial post-flash value) with overlaid best fits of pseudo first-order decays to a residual floor; inset, Stern–Volmer plot giving an apparent bimolecular rate constant of $6.0 \times 10^7 \, M^{-1} s^{-1}$. For further explanation, see the text.
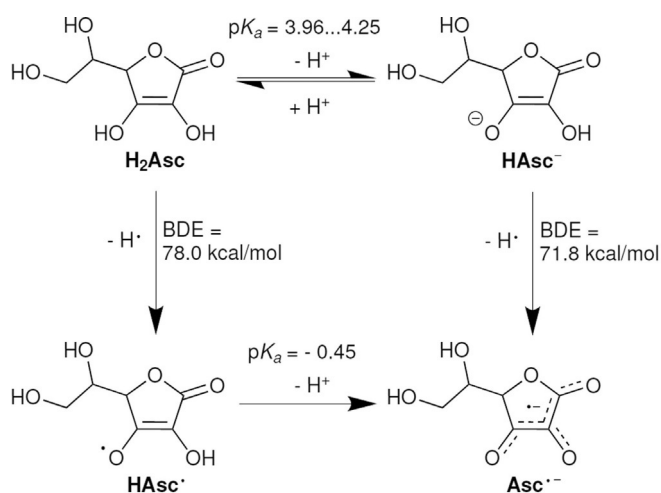


**Scheme 1.** Relations between the ascorbate-derived species relevant for this work, with $pK_a$ values[37–39] and bond dissociation energies (BDEs)[39] taken from the literature.

coefficient of $Asc^{\bullet-}$; and the constant of proportionality is the same as that between the initial absorption and the extinction coefficient of $Q^{\bullet-}$ in the 560 nm trace.

The extinction coefficients obtained by this second calibration procedure (standard, $Asc^{\bullet-}$) and by the above-described first one (standard, $e^{\bullet-}_{aq}$) differ by 2% only. This consistency not only lends support to the much higher value herein compared to the literature[19] but also, and far more importantly, establishes that $Q^{\bullet-}$ is exclusively formed through photoionization and not to any significant degree through homolytic photo-cleavage of the O—H bond.

Even though the maximum of the $Q^{\bullet-}$ absorption band (560 nm) intuitively appears best suited for observation, two considerations were instrumental for our choice of a shorter monitoring wavelength for all further experiments of this Section, namely, 515 nm. First, the sensitivity of our detection system is noticeably higher at 515 nm; and second, the dy-

namic range of the detection signal is better equalized at 515 nm when the pH is varied (compare the spectra of $HQ^{\bullet}$ and $Q^{\bullet-}$ in Figure 2a). By control experiments, we established that the decay curves at the two wavelengths are linear functions to one another.

On the basis of the first-order intrinsic decay (Figure 2b), the repair is expected to obey Stern–Volmer kinetics. Figure 4b illustrates that this surmise holds true, and that the pseudo first-order rate constant $k_{obs}$ at constant pH is a linear function of the ascorbate weight-in concentration $c_{Asc}$. However, the apparent bimolecular rate constant obtained from the slope in the inset is not meaningful per se, on account of a pronounced and intriguing pH dependence, which Figure 5a investigates at constant $c_{Asc}$. The relationship is seen to be a bell-shaped curve with an asymmetric tail to the side of higher pH. For improved precision, we measured $k_{obs}$(pH) in that region with a higher $c_{Asc}$ (100 mM) and recalculated it to $c_{Asc}$ of the rest of the data (5 mM) as in Figure 4b.

In the pH range from 2 to 9, the quercetin radicals can exist as $HQ^{\bullet}$ or $Q^{\bullet-}$ and ascorbate as the acid $H_2Asc$ or the monoanion $HAsc^-$; hence, four combinations of radical and co-antioxidant need to be taken into account. However, a significant involvement of the pair $HQ^{\bullet}/H_2Asc$ is immediately ruled out by the evident decrease of $k_{obs}$(pH) towards zero in acidic medium, where $HQ^{\bullet}$ and $H_2Asc$ are present practically exclusively.

By contrast, a reaction between $Q^{\bullet-}$ and $HAsc^-$ clearly takes place, as is manifest from the constant nonzero rate constant in the higher pH range where $Q^{\bullet-}$ and $HAsc^-$ are the only protonation forms. This process adds a contribution $k'$(pH) to $k_{obs}$, [Eq. (1)]

$$k'(\text{pH}) = k_{dep} \times \frac{1}{1 + 10^{pK_{a1} - \text{pH}}} \times \frac{1}{1 + 10^{pK_{a2} - \text{pH}}} \quad (1)$$

where $k_{dep}$—the true, pH-independent rate constant of the reaction between $Q^{\bullet-}$ and $HAsc^-$—constitutes the upper limit of

Chemistry–A European Journal

Full Paper
doi.org/10.1002/chem.202001956

**Chemistry**
**Europe**

European Chemical
Societies Publishing

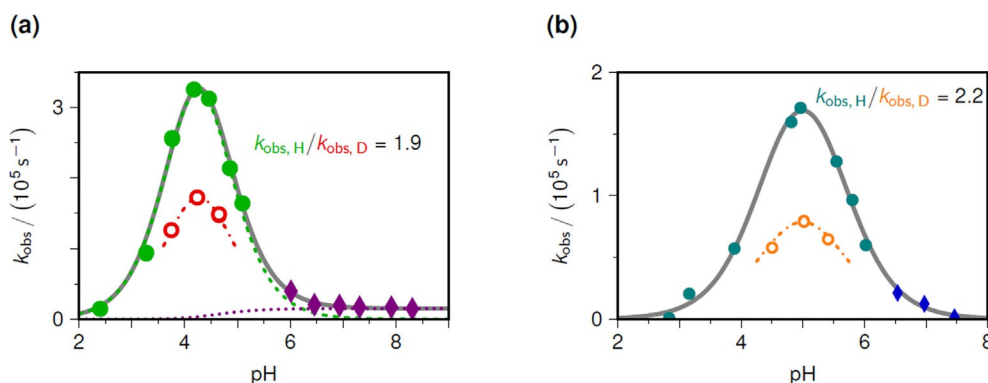**Figure 5.** Influence of pH and isotope substitution on the repair of the quercetin radicals (initial concentration, about $2\,\mu M$) by the co-antioxidants ascorbate (graph (a)) and 4-aminophenol (graph (b)) in homogeneous aqueous solution, observation at 515 nm. Shown are the observed pH-dependent pseudo first-order rate constants $k_{obs}$ at constant co-antioxidant weight-in concentration (circles, 5 mM; diamonds, 100 mM (a) and 50 mM (b), both recalculated to 5 mM). The solid gray curves are the best fits: (a), composed of Equations (1) and (4), with the individual contributions displayed as dashed green and dotted magenta curves; (b) Equation (4) only. Fixed parameter, $pK_{a1}$, 4.50. Best-fit parameters in (a) and (b): $pK_{a2}$, 4.02 and 5.51; $k'$, $1.5\times10^4\,s^{-1}$ and not applicable in the case of (b); $k$, $8.05\times10^5\,s^{-1}$ and $3.02\times10^6\,s^{-1}$. Open circles and dashed-dotted curves, experiments in $D_2O$ under otherwise identical conditions, with limited pD variation and fit for bracketing the maximum and ensuring equal vertical scaling factor [Eq. (5)]. For further explanation, see the text.

$k'(pH)$, which is approached at high pH. Equation 1 is seen to remain invariant when $pK_{a1}$ and $pK_{a2}$ are interchanged; its plot is virtually indistinguishable from a titration curve characterized by the higher of the two $pK_a$ values as long as $|pK_{a1}-pK_{a2}|$ is larger than about 1.5; and when that absolute difference becomes smaller, the mid-point slightly shifts to higher pH, with a maximum deviation of 0.4 pH units being reached for identical $pK_a$ values.

The two "mixed" reactions, between one protonated and one deprotonated species, are indistinguishable by their pH dependence: in terms of the average $\overline{M}$ and the half-difference $\overline{\Delta}$ of the two $pK_a$ values [Eq. (2), Eq. (3)]

$$\overline{M} = \frac{pK_{a1} + pK_{a2}}{2} \tag{2}$$

$$\overline{\Delta} = \frac{pK_{a1} - pK_{a2}}{2} \tag{3}$$

their rate constant $k(pH)$ can be formulated to give [Eq. (4)]

$$k(pH) = k_{mix} \times \frac{1}{1 + 10^{pH-pK_{a1}}} \times \frac{1}{1 + 10^{pK_{a2}-pH}} = k_{mix} \times \frac{10^{\overline{\Delta}}}{10^{\overline{\Delta}} + 10^{-\overline{\Delta}} + 10^{\overline{M}-pH} + 10^{pH-\overline{M}}} \tag{4}$$

The invariance of the denominator of the final expression with respect to an interchange of $pK_{a1}$ and $pK_{a2}$ is obvious. Equation (4) has been set up for species 1 reacting in its protonated form and species 2 in its deprotonated form, but an interchange of the two species, tantamount to an interchange of the two $pK_a$ values, thus merely leads to a scaling of the numerator that cannot be separated from a different value of $k_{mix}$.

To determine whether $k_{mix}$ is the pH-independent rate constant of the reaction between $HQ^\bullet$ and $HAsc^-$ or that between $Q^{\bullet-}$ and $H_2Asc$ (or a superposition of the two) and thereby to extract its correct numerical value, arguments outside mathematics have to be invoked. Fortunately, this is straightforward

in our system because $HAsc^-$ is a far better antioxidant than is $H_2Asc$ (compare the bond dissociation energies BDE in Scheme 1). Hence, we assign the mixed process exclusively to the repair of $HQ^\bullet$ by $HAsc^-$. Even without knowledge of the BDE, this is entirely consistent with it being much faster than the high-pH repair of $Q^{\bullet-}$ by $HAsc^-$, meaning that $HQ^\bullet$ is more reactive than is $Q^{\bullet-}$ and implying that a reaction between $Q^{\bullet-}$ and $H_2Asc$ would be slower than the already unobservable one between $HQ^\bullet$ and $H_2Asc$.

Equations (1) and (4) share the same $pK_a$ values, one of which (the $pK_a$ of $HQ^\bullet$) was determined herein under exactly the same experimental conditions. Because of considerable spread in the reported $pK_a$ of $H_2Asc$ (between $3.96^{[37]}$ and $4.25^{[38]}$), we treated that parameter as adjustable, in addition to $k_{dep}$ and $k_{mix}$. The resulting three-parameter best fit of the sum of Equations (1) and (4) to $k_{obs}(pH)$ is displayed in Figure 5a. As emerges from the separated contributions that have also been plotted, the fit is extremely well-conditioned because $k_{dep}$ can practically be read off from the data in the region of high pH. The fit converged near the lower of the two $pK_a$ values of $H_2Asc$ cited above; and dividing $k_{mix}$ and $k_{dep}$ by $c_{Asc}$ finally yielded the true second-order rate constants, $1.6\times10^8\,M^{-1}s^{-1}$ and $3.0\times10^6\,M^{-1}s^{-1}$ for the reactions of $HAsc^-$ with $HQ^\bullet$ and with $Q^{\bullet-}$.

Only two kinetic investigations on fast timescales were carried out on quercetin/ascorbate systems so far, and both were performed at a single pH only, $8.5^{[18]}$ or $10.8.^{[19]}$ The latter work lists a rate constant of $2.4\times10^5\,M^{-1}s^{-1}$ but, according to the authors' conclusions, the quercetin radicals are doubly deprotonated at pH 10.8 (second $pK_a$, 9.4); hence, that rate constant applies to a reaction different from ours. From a highly complex kinetic modelling, the former study extracts a rate constant of $5.0\times10^6\,M^{-1}s^{-1}$ for what must be the reaction between $Q^{\bullet-}$ and $HAsc^-$. Our result is 40% lower but we believe

Chemistry–A European Journal

Full Paper
doi.org/10.1002/chem.202001956

**Chemistry Europe**
European Chemical
Societies Publishing

it to be more reliable because we obtained it by direct kinetic measurements of the isolated process.

For the reaction between $HQ^{\bullet}$ and $HAsc^{-}$, no rate constant seems to have been reported to date. We stress that, in view of the bell-shaped pH dependence (Figure 5a) and its underlying formula, measurements at a single pH would have suggested values that are grossly too low: even if, through lucky coincidence, these experiments had been carried out at the maximum of the bell-shaped curve [Eq. (5)],

$$k(\mathrm{pH}=\overline{M}) \qquad = \qquad k_{\mathrm{mix}} \times \frac{10^{\overline{\Delta}}}{2 + 10^{\overline{\Delta}} + 10^{-\overline{\Delta}}} \qquad (5)$$

the $pK_a$-dependent fraction in Equation (5) would have necessitated a correction by a factor of 2.5 with our parameters ($pK_{a1} - pK_{a2} = 0.48$) to obtain $k_{\mathrm{mix}}$; this would have risen to a factor of 4 if both $pK_a$ values happened to be equal; and, from Equation (4), to much more if some pH in the outer wings of the curve had accidentally been chosen.

The regeneration of the quercetin from $HQ^{\bullet}$ could be a concerted process (proton-coupled electron transfer PCET) or a sequential one (rate-determining electron transfer followed by proton transfer, SETPT; or rate-determining proton loss followed by electron transfer, SPLET). The pertinent $pK_a$ values, 11.74 of $HAsc^{-}$ and $-0.45$ of $HAsc^{\bullet}$,[38,39] already disfavor SETPT and SPLET, and the H/D kinetic isotope effects (KIEs), which have also been included in Figure 5a, provide direct experimental evidence. SETPT could only lead to a small secondary KIE, and SPLET to a similarly small thermodynamic isotope effect on the deprotonation equilibrium of $HAsc^{-}$,[40] whereas PCET is expected to exhibit a primary KIE.

Because all hydroxylic protons of quercetin and ascorbate are exchangeable and the reagent concentrations are very small, complete deuteration at the relevant positions is achieved before the start of the photoionization in $D_2O$. Determining KIEs for a reaction with complex pH dependence faces the problem that $pK_a$ values in $H_2O$ and $D_2O$ might be slightly different; and the same applies to pH and pD readings. Potential pitfalls are thus comparing data at the maximum of the curve (Figure 5a) in one solvent with off-maximum data in the other solvent; and, independent from the former, overlooking different trailing fractions in Equation (5) caused by a discrepancy of $\overline{\Delta}$ in the two solvents. To avoid these sources of errors, we carried out a limited pD variation to localize the maximum in $D_2O$ and to ensure that the width of the bell-shaped dependence, which is only related to $\overline{\Delta}$ but not to $\overline{M}$, does not change. Figure 5a displays the outcome, which gave the same $\overline{\Delta}$ in $D_2O$ and apparently also the same $\overline{M}$ as in $H_2O$. Although the latter might well be due to an equal influence of the deuterated solvent on the potential of the glass electrode, Equation (4) is insensitive to such a shift of the horizontal scale as a whole. Direct comparison of the maxima yields a KIE of 1.9, whose magnitude can only be reconciled with a primary KIE and thus the PCET mechanism.[40]

Only an estimate can be given for the KIE in basic medium because the reaction in $D_2O$ becomes so slow that the correction for the decay without 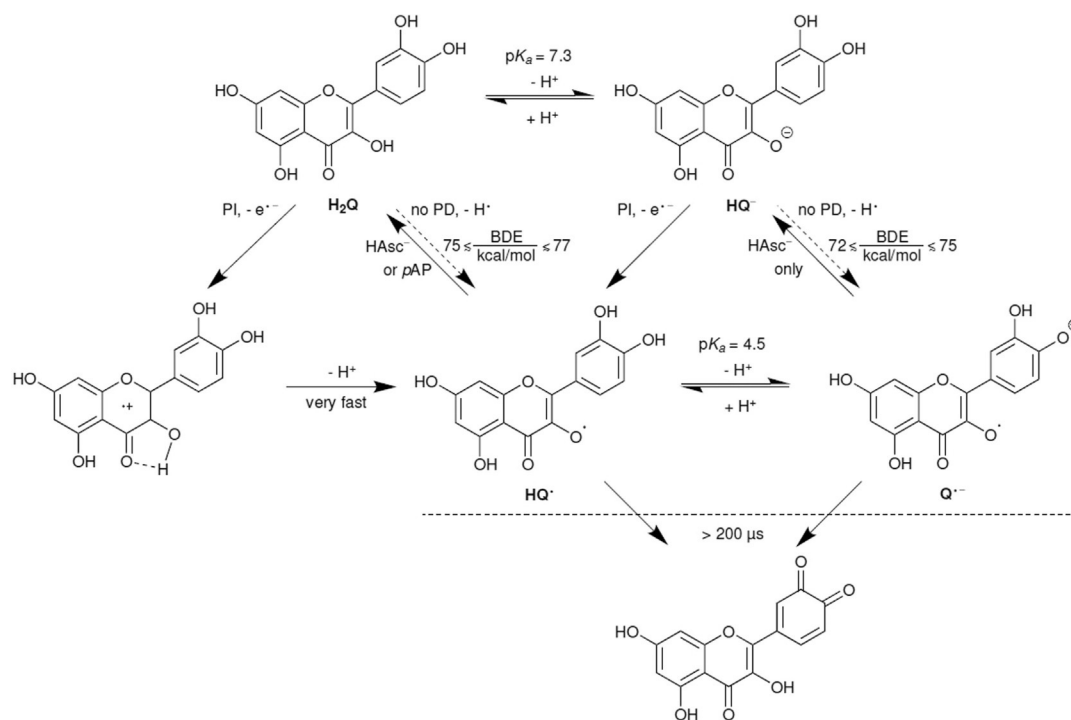quencher (compare, Figure 2b) entails a rather large error. Single-point measurements at pH 8.0 gave a KIE between 3 and 5, which suggests a PCET mechanism for the repair of $Q^{\bullet-}$ by $HAsc^{-}$ as well.

Theoretical investigations report bond dissociation energies (BDEs) in aqueous solution between 71.3 kcal mol$^{-1}$ and 83.1 kcal mol$^{-1}$ for $H_2Q$,[32,35] and between 70.9 kcal mol$^{-1}$ and 75.0 kcal mol$^{-1}$ for $HQ^{-}$.[32,35] Precise experimental values are unavailable, but our results of Figure 5a allow bracketing these key quantities, in particular that of $H_2Q$ with a much lower uncertainty. A PCET is thermodynamically feasible when the BDE of the co-antioxidant is smaller than the BDE of the regenerated quercetin, each in its respective protonation state. The combination of no discernible repair of the quercetin radicals by $H_2Asc$ (BDE, 78.0 kcal mol$^{-1}$)[39] and successful repairs by $HAsc^{-}$ (BDE, 71.8 kcal mol$^{-1}$)[39] thus puts a first upper and lower limit on the BDEs of $H_2Q$ and $HQ^{-}$; in full accordance with this, we found reduced glutathione (BDE, 87.2 kcal mol$^{-1}$)[39] to be inoperative as a repairing agent; the upper boundary is substantiated and even slightly tightened by our observations that neither hydroquinone (BDE, 79.7 kcal mol$^{-1}$)[39] nor a water-soluble analogue of $\alpha$-tocopherol (Trolox; BDE, 76.7 kcal mol$^{-1}$)[39] are capable of repairing the quercetin radicals in the pH range of Figure 5a, where no deprotonations of the co-antioxidant hydroxylic groups need to be taken into account; and our following experiments (Figure 5b), which demonstrate that $p$-aminophenol $p$AP (BDE, 75.0 kcal mol$^{-1}$)[39] can repair $HQ^{\bullet}$ but not $Q^{\bullet-}$, both raise the lower limit for $H_2Q$ and decrease the upper limit for $HQ^{-}$ still further.

The deprotonation of the phenolic OH-group of $p$AP falls outside the pH range investigated, but the amino group already becomes protonated in slightly acidic medium ($pK_a$, 5.48),[41] whereby this phenol loses its good antioxidant properties. In line with expectation, no repair is thus observed at low pH, where only $HQ^{\bullet}$ and N-protonated $p$AP exist. When the pH is raised, the increase of available co-antioxidant through deprotonation at N is countered by the transformation of $HQ^{\bullet}$ into the less readily repaired $Q^{\bullet-}$, such that again a bell-shaped pH dependence of $k_{\mathrm{obs}}$ results. On its high-pH side, however, no constant floor is detectable; hence, no repair of $Q^{\bullet-}$ by $p$AP occurs.

As the main difference to the ascorbate case of Figure 5a, $\overline{\Delta}$ [Eq. (3)] is negative for $HQ^{\bullet}/p$AP. From the above discussion it emerges that this does not influence the shape of the pH dependence in any way. However, it strongly decreases the scale factor given by Equation (5) such that the curve at its maximum amounts to less than 6% of $k_{\mathrm{mix}}$ only, whereas that factor was seven times higher for $HQ^{\bullet}/HAsc^{-}$. The resulting lower $k_{\mathrm{obs}}$ thus totally masks that the true rate constant for the repair of $HQ^{\bullet}$ by $p$AP, $6.0 \times 10^8 \mathrm{M}^{-1} \mathrm{s}^{-1}$, is about four times larger than that with the co-antioxidant $HAsc^{-}$. We stress that this difference is not due to a change of mechanism: the KIE of 2.2 in Figure 5b, which was obtained by the same procedure as before, confirms that the reaction remains a PCET when $p$AP replaces $HAsc^{-}$.

Despite the lower thermodynamic driving force, $p$AP repairs $HQ^{\bullet}$ faster than does $HAsc^{-}$. We have already observed the same phenomenon for the repairs of the resveratrol radical by

**Chemistry–A European Journal**

Full Paper
doi.org/10.1002/chem.202001956

**Chemistry Europe**
European Chemical
Societies Publishing

**Scheme 2.** Quercetin-derived species[35] with their abbreviations; connecting pathways pertinent to this work, p$K_a$ values, and bond dissociation energies BDE, as determined herein.

these two co-antioxidants.[20] Most likely, steric constraints on the highly ordered PCET transition state provide the underlying reason.

The findings of this work regarding the pathways to the quercetin radicals HQ• and Q•−, the feasibility or infeasibility of their repairs by co-antioxidants, and the derived intervals for the BDEs of H$_2$Q and HQ− have been collected in Scheme 2.

## Conclusions

As has emerged, flash photolysis with an inexpensive near-UV pulsed solid-state laser (355 nm) provides an extremely convenient access to quercetin radicals through photoionization. In fact, not a single additive is needed per se, although as a variant one can blank out the only by-product e$_{aq}^{•−}$ by saturating the solution with N$_2$O. Neither e$_{aq}^{•−}$ nor its blanking product HO• interfere with residual quercetin or its radicals for kinetic reasons; the timescale of the radical generation is set by the duration of the laser flash, a few ns, which is tantamount to instantaneous generation when typical secondary reactions with co-antioxidants on µs timescales are studied; and within a wide pH range (between 2–3 and 9), the attainable post-flash radical concentration is up to one-half the substrate concentration while being easily controlled by the laser power.

Besides allowing a characterization of the neutral and anion radicals HQ• and Q•−, including a recalibration of their absorption spectra with very different results compared to the literature, the photoionization approach paved the way to a detailed study of the interactions of HQ• and Q•− with the ascorbate monoanion HAsc− and other co-antioxidants, such as 4-

aminophenol. Most conspicuous were the bell-shaped pH dependences of the repair kinetics of HQ•, in consequence of which the maxima of the observed rate constants as functions of the pH represent only a fraction of the true rate constants for the repair of HQ• by the co-antioxidant, such that single-point measurements even at the exact maxima could be grossly misleading. Given that we were able to identify the repair mechanisms as proton-coupled electron transfers, a comparison of different co-antioxidants with known bond dissociation energies allowed us to specify the bond dissociation energies of quercetin and its monoanion with much smaller uncertainties than previously estimated by quantum-mechanical calculations.

On the basis of the Stern–Volmer behavior of the repairs with ascorbate, the 50 times lower reactivity of the quercetin radical anion compared to the neutral radical, and a p$K_a$ value of the latter below 5, it is evident that no complete repair is achievable with reasonable ascorbate concentrations at physiological pH in homogeneous solution. However, that pessimistic picture should no longer be valid in organized systems; and we envisage that our laser flash photolysis approach, which generates the radicals at the exact locations of their precursors, will prove useful in such situations, as we have already shown in the case of the antioxidant resveratrol and its repairs through micelle–water interfaces.[42]

## Acknowledgements

## Conflict of interest

The authors declare no conflict of interest.

[1]   C. A. Rice-Evans, N. J. Miller, P. G. Bolwell, P. M. Bramley, J. B. Pridham, *Free Radic. Res.* **1995**, *22*, 375 – 383.

[2]   A. J. Larson, J. D. Symons, T. Jalili, *Adv. Nutr. Res.* **2012**, *3*, 39 – 46.

[3]   S. Egert, A. Bosy-Westphal, J. Seiberl, C. Kuerbitz, U. Settler, S. Plachta-Danielzik, A. E. Wagner, J. Frank, J. Schrezenmeir, G. Rimbach, S. Wolfram, M. J. Müller, *Br. J. Nutr.* **2009**, *102*, 1065 – 1074.

[4]   S. C. Bischoff, *Curr. Opin. Clin. Nutr. Metab. Care* **2008**, *11*, 733 – 740.

[5]   Y. J. Moon, X. Wang, M. E. Morris, *Toxicol. in Vitro* **2006**, *20*, 187 – 210.

[6]   T. T. H. Nguyen, S.-H. Yu, J. Kim, E. An, K. Hwang, J.-S. Park, D. Kim, *Funct. Food Health Dis.* **2015**, *5*, 437 – 449.

[7]   S. Jo, H. Kim, S. Kim, D. H. Shin, M. S. Kim, *Chem. Biol. Drug Des.* **2019**, *94*, 2023 – 2030.

[8]   X. Qiu, A. Kroeker, S. He, R. Kozak, J. Audet, M. Mbikay, M. Chrétien, *Antimicrob. Agents Chemother.* **2016**, *60*, 5182 – 5188.

[9]   G. Wong, S. He, V. Siragam, Y. Bi, M. Mbikay, M. Chrétien, X. Qiu, *Virol. Sin.* **2017**, *32*, 545 – 547.

[10]   C. Sargiacomo, F. Sotgia, M. P. Lisanti, *Aging* **2020**, *12*, 6511 – 6517.

[11]   L. Choueiri, V. S. Chedea, A. Calokerinos, P. Kefalas, *Food Chem.* **2012**, *133*, 1039 – 1044.

[12]   R. Vrijsen, L. Everaert, A. Boeyé, *J. Gen. Virol.* **1988**, *69*, 1749 – 1751.

[13]   C. Kandaswami, E. Perkins, D. S. Soloniuk, G. Drzewiecki, E. Middleton, *Anti-Cancer Drugs* **1993**, *4*, 91 – 96.

[14]   G. Galati, O. Sabzevari, J. X. Wilson, P. J. O'Brien, *Toxicology* **2002**, *177*, 91 – 1043.

[15]   E. Atala, J. Fuentes, M. J. Wehrhahn, H. Speisky, *Food Chem.* **2017**, *234*, 479 – 485.

[16]   J. Fuentes, E. Atala, E. Pastene, C. Carrasco-Pozo, H. Speisky, *J. Agric. Food Chem.* **2017**, *65*, 11002 – 11010.

[17]   A. Vásquez-Espina, O. Yañez, E. Osorio, C. Areche, O. García-Beltrán, L. M. Ruiz, B. K. Cassels, W. Tiznado, *Front. Chem.* **2019**, *7*, 818.

[18]   W. Bors, C. Michel, S. Schikora, *Free Radic. Biol. Med.* **1995**, *19*, 45 – 52.

[19]   S. V. Jovanovic, S. Steenken, Y. Hara, M. G. Simic, *J. Chem. Soc. Perkin Trans 2* **1996**, 2497 – 2504.

[20]   C. Kerzig, S. Henkel, M. Goez, *Phys. Chem. Chem. Phys.* **2015**, *17*, 13915 – 13920.

[21]   M. Goez, C. Kerzig, R. Naumann, *Angew. Chem. Int. Ed.* **2014**, *53*, 9914 – 9916; *Angew. Chem.* **2014**, *126*, 10072 – 10074.

[22]   T. Momić, J. Z. Savić, U. Černigoj, P. Trebse, V. Vasić, *Collect. Czechoslov. Chem. Commun.* **2007**, *72*, 1447 – 1460.

[23]   K. Lemańska, H. van der Woude, H. Szymusiak, M. G. Boersma, A. Gliszczyńska-Świgło, I. M. Rietjens, B. Tyrakowska, *Free Radic. Res.* **2004**, *38*, 639 – 647.

[24]   J. R. Lakowicz, *Principles of Fluorescence Spectroscopy*, 3rd ed., Springer, New York, **2006**.

[25]   G. V. Buxton, C. L. Greenstock, W. P. Heiman, A. B. Ross, *J. Phys. Chem. Ref. Data* **1988**, *17*, 513 – 886.

[26]   M. Brautzsch, C. Kerzig, M. Goez, *Green Chem.* **2016**, *18*, 4761 – 4771.

[27]   F. Di Meo, V. Lemaur, J. Cornil, R. Lazzaroni, J.-L. Duroux, Y. Olivier, P. Trouillas, *J. Phys. Chem. A* **2013**, *117*, 2082 – 2092.

[28]   K. Lemańska, H. Szymusiak, B. Tyrakowska, R. Zieliński, A. E. Soffers, I. M. Rietjens, *Free Radic. Biol. Med.* **2001**, *31*, 869 – 881.

[29]   A. Zhou, O. A. Sadik, *J. Agric. Food Chem.* **2008**, *56*, 12081 – 12091.

[30]   C. Kerzig, M. Goez, *Phys. Chem. Chem. Phys.* **2015**, *17*, 13829 – 13836.

[31]   J.-C. Mialocq, J. Sutton, P. Goujon, *J. Chem. Phys.* **1980**, *72*, 6338 – 6345.

[32]   D. Amić, V. Stepanić, B. Lučić, Z. Marković, J. M. Dimitrić Marković, *J. Mol. Model.* **2013**, *19*, 2593 – 2603.

[33]   L. Lu, M. Qiang, F. Li, H. Zhang, S. Zhang, *Dyes Pigm.* **2014**, *103*, 175 – 182.

[34]   Y.-Z. Zheng, G. Deng, Q. Liang, D.-F. Chen, R. Guo, R.-C. Lai, *Sci. Rep.* **2017**, *7*, 7543 – 7553.

[35]   R. Amorati, A. Baschieri, A. Cowden, L. Valgimigli, *Biomimetics* **2017**, *2*, 9 – 21.

[36]   U. Lachish, A. Shafferman, G. Stein, *J. Chem. Phys.* **1976**, *64*, 4205 – 4211.

[37]   M. Kimura, M. Yamamoto, S. Yamabe, *J. Chem. Soc. Dalton Trans.* **1982**, 423 – 427.

[38]   M. B. Davies, J. Austin, D. A. Partridge, *Vitamin C: Its Chemistry and Biochemistry*, 1st ed., The Royal Society of Chemistry, Cambridge, **1991**.

[39]   J. J. Warren, T. A. Tronic, J. M. Mayer, *Chem. Rev.* **2010**, *110*, 6961 – 7001.

[40]   I. J. Rhile, T. F. Markle, H. Nagao, A. G. DiPasquale, O. P. Lam, M. A. Lockwood, K. Rotter, J. M. Mayer, *J. Am. Chem. Soc.* **2006**, *128*, 6075 – 6088.

[41]   *CRC Handbook of Chemistry and Physics*, 97th ed. (Ed.: W. M. Haynes), CRC press, Boca Raton, **2016**.

[42]   C. Kerzig, M. Hoffmann, M. Goez, *Chem. Eur. J.* **2018**, *24*, 3038 – 3044.